Journal of Microscopy and Ultrastructure 3 (2015) 8–18

Contents lists available at ScienceDirect

Journal of Microscopy and Ultrastructure

journal homepage: www.elsevier.com/locate/jmau

Original Article

The effect of manganese on the olfactory bulb of adult male albino rat and the role of meloxicam: A histological and immunohistochemical study

Amany M. Mousa[a,*], Amal A. Shehab[b]

[a] Histology Department, Faculty of Medicine, Tanta University, Egypt
[b] Anatomy & Embryology Department, Faculty of Medicine, Tanta University, Egypt

ARTICLE INFO

Article history:
Received 9 September 2014
Received in revised form 6 November 2014
Accepted 11 November 2014
Available online 18 November 2014

Keywords:
Olfactory bulb
$MnCl_2$
Meloxicam
Ultrastructure
Glial fibrillary acid protein (GFAP)

ABSTRACT

Manganese (Mn) is an essential metal commonly found in the environment and is used for industrial purposes. Exposure to excessively high Mn levels may induce neurotoxicity referred to as manganism. This work was conducted to study the effect of manganese on the olfactory bulb of adult male albino rat and the possible protective role of meloxicam. Forty adult male albino rats were equally divided into four groups: control group, meloxicam-treated group (5 mg/kg/day orally for 4 weeks), $MnCl_2$-treated group (10 mg/kg/day orally for 4 weeks), and the fourth group received both meloxicam and $MnCl_2$ at the same doses and duration. Specimens of the olfactory bulbs were prepared for light and electron microscopy. An immunohistochemical study with a quantitative morphometry was performed using antibodies against glial fibrillary acidic protein (GFAP). The control group and meloxicam-treated group showed the same normal structure. $MnCl_2$-treated group showed shrinkage of mitral nerve cells with dark peripheral nuclei as well as disorganization of mitral and granule nerve cells. The surrounding neuropil showed vacuolar spaces. Ultrastructurally, the mitral cells showed accumulation of lysosomes, swelling of mitochondria and irregularity of the nuclei. The nerve fibers contained swollen mitochondria with splitting and irregularity of the surrounding myelin sheaths. GFAP immunoreaction showed a highly significant increase compared to control group. On the other hand, the group that received both meloxicam and $MnCl_2$ showed less marked histological changes. It was concluded that manganese induced structural changes in the olfactory bulb of albino rat that were ameliorated by concomitant use of meloxicam.

1. Introduction

Manganese (Mn) is a naturally occurring trace element, critical for optimal functions of different organs [1]. It participates in numerous enzymatic reactions such as hydrolases, kinases, decarboxylases and transferases. In addition, it acts as a co-factor for a series of enzymes involved in both lipid and carbohydrate metabolism [2,3]. Deficiency or excessive exposure to this metal may lead to various health disorders [4].

Environmental contamination by Mn may occur as a result of its use for industrial purposes including the manufacture of steel, iron, glass ceramics and fertilizers [5]. It is also used in the manufacture of paints, soaps, batteries and insecticides. Both mine and metal workers are frequently exposed to Mn [6]. Increased levels of Mn have been also

* Corresponding author. Tel.: +20 01005475496.
E-mail address: amanymousa2003@gmail.com (A.M. Mousa).

http://dx.doi.org/10.1016/j.jmau.2014.11.002
2213-879X/

detected in individuals ingesting contaminated well-water and parenteral nutrition therapy [7]. These environmental, occupational and disease conditions lead to excessive Mn accumulation in the nervous system [8]. It was recorded that Mn may cause intoxication in humans exposed to high concentrations of this metal or to low doses for long periods of time [9].

The pulmonary route is the main entrance of Mn into the body. However, the brain can retain it for longer periods of time than other organs, probably due to its inability to get rid of the excess of this metal. Manganese may cross the blood brain barrier and is delivered to different brain regions via an axonal transport system [6]. It was reported that exposure to high levels of Mn may cause an irreversible brain disease referred to as manganism, with symptoms similar to those in Parkinson's disease [10].

Several antioxidants have been reported to reduce the oxidative stress occurring during neurotoxicity. Non-steroidal anti-inflammatory drugs (NSAIDs) are the group of drugs with anti-inflammatory, analgesic and antipyretic activities that work by interfering with the cyclooxygenase (COX) pathway. They inhibit the enzyme COX which is responsible for converting arachidonic acid into prostaglandin H2 which is a mediator of inflammation [11]. NSAIDs have an antioxidant property and have been shown to improve the circulating antioxidant status in different diseases [12–14].

Meloxicam is a NSAID that appears to have a selective inhibitory activity against the inducible isoform cyclooxygenase-2 (COX-2), than against the constitutive isoform cyclooxygenase-1 (COX-1). It was found that inhibition of COX-1 is associated with gastrointestinal, renal, and platelet aggregation adverse effects. Therefore, meloxicam and other COX-2 selective inhibitors are promoted for their safer profile of side effects. They reduce prostaglandin biosynthesis without interference to the same extent with the normal functions and mucosal protective activities mediated by COX-1 [11]. Moreover, meloxicam has a significant antioxidant role that has been reported in aluminum-induced oxidative stress in rat brain [14].

The olfactory bulb is one of the structures located in the limbic region of the brain. It is an oval mass that lies below the anterior end of the olfactory sulcus. The olfactory bulb is supported and protected by the cribriform plate of the ethmoid bone, which in mammals separates it from the olfactory epithelium, and which is perforated by olfactory nerve axons. The olfactory bulb consists of a collection of nerve cells that receives impulses from the olfactory nerves of the nasal mucosa and continues as the olfactory tract [15].

This research was designed to study the effect of manganese chloride ($MnCl_2$) on the structure of olfactory bulb of adult male albino rat and the possible role of meloxicam as a protective agent against $MnCl_2$ neurotoxicity using light and electron microscopes. In addition, an immunohistochemical technique was also performed using antibodies against glial fibrillary acidic protein (GFAP) which is an intermediate filament protein found in the cytoskeleton of astrocytes and was used as a marker for astrogliosis [16].

2. Materials and methods

The present work was carried out on 40 adult male albino rats weighing 180–200 g each. They were housed in clean properly ventilated cages, maintained on a 12:12-h dark–light cycle and provided with balanced food and water. The animals were acclimatized for 10 days before the beginning of the experiment and the general condition of the animals was checked daily. They were randomly distributed into four groups (10 animals each):

Group I (control group): the animals were divided into two subgroups: five rats were left without treatment and five rats each was given 1 ml of sterile saline each, orally by a gastric tube once daily for 4 weeks.
Group II: each animal was given meloxicam (5 mg/kg body weight) [14] dissolved in 1 ml of sterile saline orally by a gastric tube once daily for 4 weeks. Meloxicam (Anti-Cox II) was manufactured by ADWIA Company (10th of Ramadan City, Egypt) in the form of tablets containing 15 mg each.
Group III: each animal was given $MnCl_2$ (10 mg/kg body weight) [3,17] dissolved in 1 ml of sterile saline orally by a gastric tube once daily for 4 weeks. $MnCl_2$ was purchased from El-Faraana Chemical Company (Tanta, Egypt) in the form of a powder.
Group IV: the animals were concomitantly given both meloxicam and $MnCl_2$ at the same doses and duration as in groups II and III.

At the end of the experiment, all animals were anesthetized by intraperitoneal injection of sodium pentobarbital (30 mg/kg body weight) [18]. Following perfusion through the left ventricle of the heart with a fixative containing 2.5% glutaraldehyde and 4% paraformaldehyde in 0.1 M phosphate buffer at pH 7.4, the brains were immediately extracted, and the olfactory bulbs were dissected out.

For light microscopy, the specimens were fixed in 10% neutral-buffered formalin, dehydrated through ascending grades of ethanol, cleared in xylene and infiltrated and embedded in paraffin wax. Then, sections (5 μm thick) were cut and stained with hematoxylin and eosin (H&E) [19].

For immunohistochemistry, GFAP was performed on formalin-fixed paraffin-embedded specimens. The tissue sections were deparaffinized, rehydrated and incubated for 30 min with 3% hydrogen peroxide for inhibition of endogenous peroxidase. The slides were rinsed in phosphate buffered saline (PBS) and incubated overnight at 4 °C with anti-GFAP antibody (NeoMarkers/Lab Vision, Fremont, CA, USA). Sections were then rinsed in PBS, incubated for 1 h with biotinylated peroxidase-conjugated secondary antibody. In the next step, sections were rinsed in PBS and incubated with diaminobenzidine (DAB) for visualization of the immunoreaction. The sections were then rinsed in PBS, counterstained with Mayer's hematoxylin, dehydrated and mounted. The negative control sections were incubated with normal serum instead of the primary antibody, while other steps of the procedure were the same [20,21].

For electron microscopy, the specimens were immersed for 2 h in 2.5% phosphate buffered glutaraldehyde solution (pH 7.4) at 4 °C. After washing with phosphate buffer, the specimens were post-fixed for 1 h in 1% buffered osmium tetroxide solution. Subsequently, the specimens were dehydrated and cleared in acetone and were embedded in epoxy resin. Semithin sections (1 μm) were stained by 1% toluidine blue for proper orientation. Ultrathin sections (70 nm) were cut with a diamond knife on a LEICA ultratome (Austria), double-stained with uranyl acetate and lead citrate [22], and were examined with a JEOL electron microscope (Tokyo, Japan) at EM unit, Tanta University.

2.1. Quantitative morphometric study

Regarding GFAP immunoreactivity, 10 different fields were randomly examined from each animal at a magnification of 400 and the area percentage of the immunoreaction was measured using an image analyzer computer system.

All quantitative data were expressed as means (X) ± standard deviation (SD). Statistical analysis using Student's t-test was carried out to compare each group with the control group. P value was calculated using Statistical Package for Social Sciences (SPSS, version 11.5, Chicago, USA) statistical analysis software. The results were considered statistically significant when P value was less than 0.05 and highly significant when P value was less than 0.001.

3. Results

3.1. Light microscopic results

H&E-stained sections of the olfactory bulb obtained from the control group (group I) showed normal six laminae from outside inwards: olfactory nerve layer, glomerular layer, external plexiform layer, mitral cell layer, internal plexiform layer and granular cell layer. The olfactory nerve layer contained nerve fibers and scattered supporting cells. In the glomerular layer, glomeruli were observed; each of them was surrounded by a rim of periglomerular cells. The external plexiform layer consisted of nerve fibers and some neurons having dark nuclei (Fig. 1). The mitral cell layer showed pyramidal shaped mitral nerve cells having abundant cytoplasm and pale vesicular nuclei with prominent nucleoli. Some granule nerve cells were observed scattered through the mitral cell layer. They appeared smaller than mitral cells with scanty cytoplasm and dark nuclei. The internal plexiform layer was adjacent to the mitral cell layer and consisting mainly of nerve fibers. In the granular cell layer, numerous granule nerve cells appeared in clusters. These granule cells were greater in number than any other type of cells observed in the olfactory bulb (Figs. 2 and 3).

Regarding GFAP-immunostained sections, few cells with positive immunoreaction in their cytoplasmic processes were observed in different layers of the olfactory bulb (Fig. 4).

It was found that meloxicam-treated group (group II) showed the same histological and immunohistochemical findings as those of the control group.

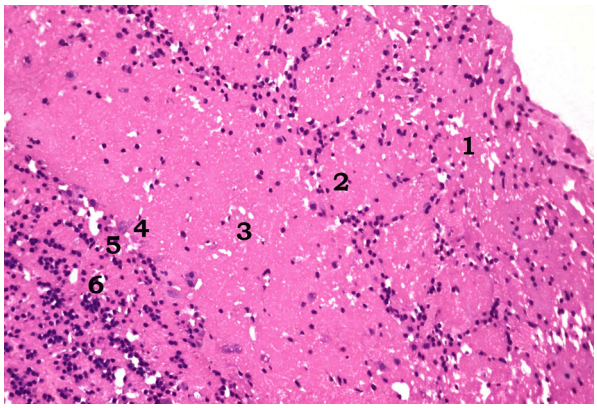

Fig. 1. A photomicrograph of a section in the olfactory bulb from the control group showing six laminae: olfactory nerve layer (1), glomerular layer (2), external plexiform layer (3), mitral cell layer (4), internal plexiform layer (5), and granular cell layer (6) (H&E, Mic. Mag. 200×).

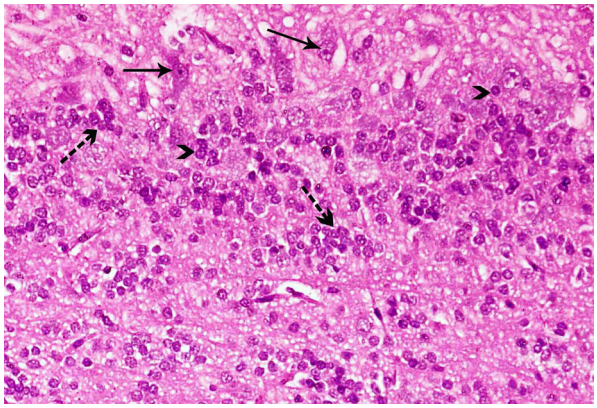

Fig. 2. A photomicrograph of a section in the olfactory bulb from the control group showing pyramidal shaped mitral nerve cells with abundant cytoplasm and vesicular nuclei (→). The granule nerve cells are rounded small cells with scanty cytoplasm and dark nuclei (>). The granule cells appear in clusters (—>) and some are scattered through the mitral cell layer (H&E, Mic. Mag. 400×).

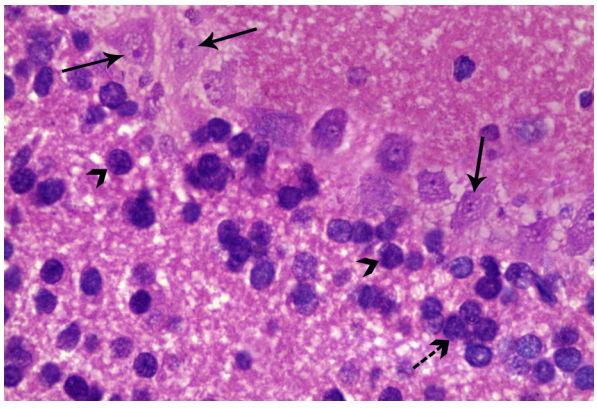

Fig. 3. A photomicrograph of a section in the olfactory bulb from the control group showing mitral nerve cells with abundant cytoplasm and vesicular nuclei (→) containing prominent nucleoli. The granule nerve cells are rounded small cells with scanty cytoplasm and dark nuclei (>). Most of the granule cells appear in clusters (—>) (H&E, Mic. Mag. 1000×).

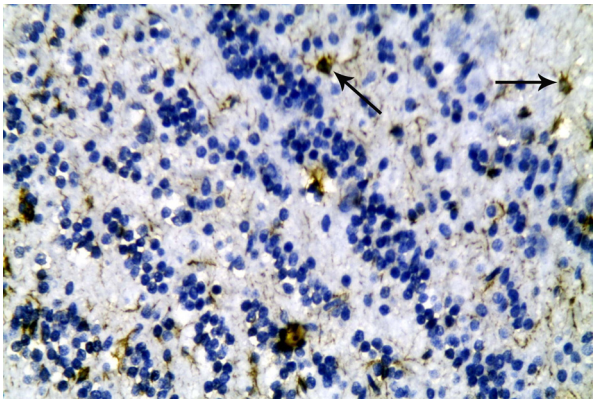

Fig. 4. A photomicrograph of a section in the olfactory bulb from the control group showing a few cells with positive immunoreaction in their processes in different layers (→) (immunostaining for GFAP, Mic. Mag. 400×).

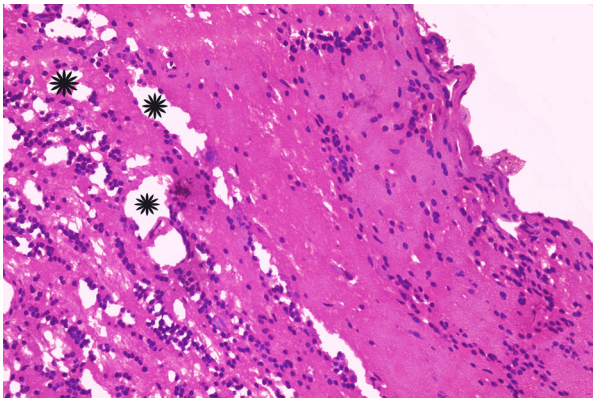

Fig. 5. A photomicrograph of a section in the olfactory bulb from $MnCl_2$-treated group (group III) showing disturbed architecture with loss of normal laminar organization as well as vacuolar spaces in the neuropil (*) (H&E, Mic. Mag 200×).

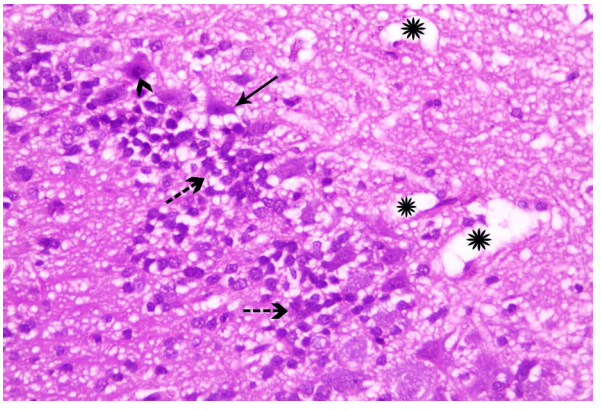

Fig. 6. A photomicrograph of a section in the olfactory bulb from group III showing darkly stained mitral cells (→) with dark pyknotic peripheral nuclei (>), disorganization of granular cell layer (–>) and vacuolar spaces in the neuropil (*) (H&E, Mic. Mag. 400×).

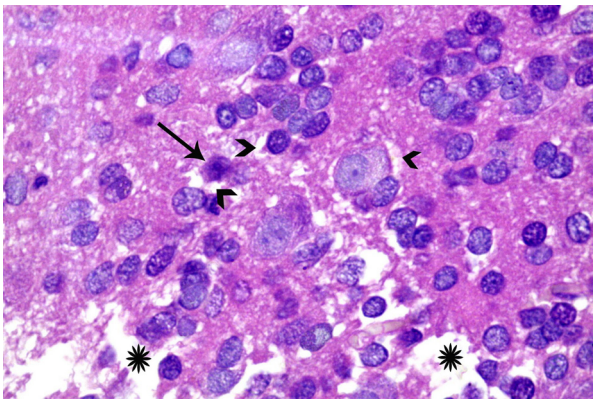

Fig. 7. A photomicrograph of a section in the olfactory bulb from group III showing some mitral nerve cells with pyknotic nuclei (→) and some show pericellular spaces (>). The neuropil shows vacuolar spaces (*) (H&E, Mic. Mag. 1000×).

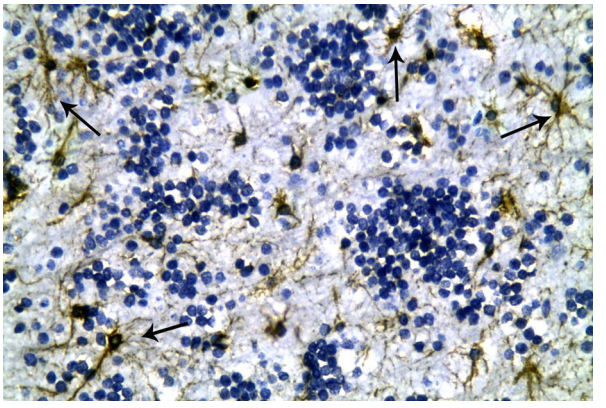

Fig. 8. A photomicrograph of a section in the olfactory bulb from group III showing a strong extensive immunoreaction in the processes of astrocytes in different layers (→) (immunostaining for GFAP, Mic. Mag. 400×).

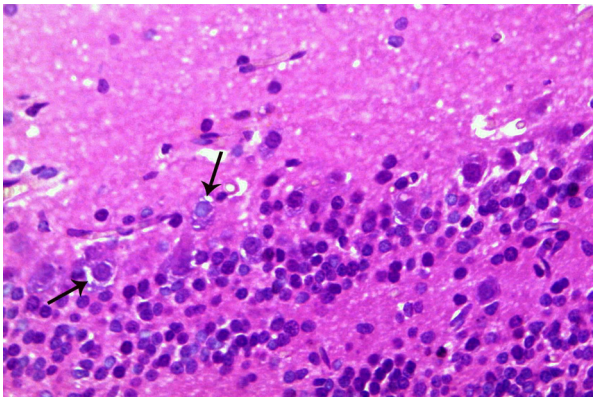

Fig. 9. A photomicrograph of a section in the olfactory bulb from meloxicam and $MnCl_2$-treated group (group IV) showing cytoplasmic vacuolation of some mitral nerve cells (→) (H&E, Mic. Mag. 400×).

As regards $MnCl_2$-treated animals (group III), disturbed architecture of the olfactory bulb was observed with loss of normal laminar organization (Fig. 5). The mitral nerve cells appeared distorted, small, and shrunken with darkly

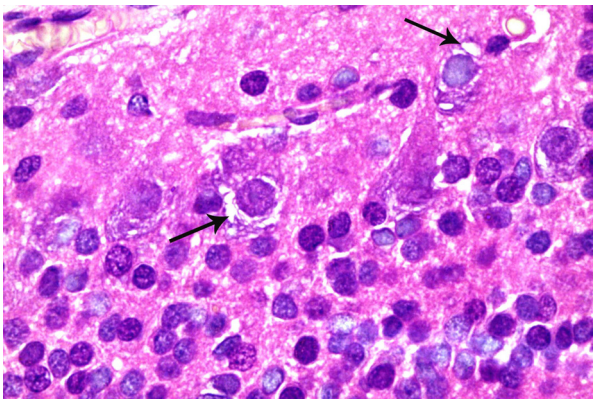

Fig. 10. A higher magnification of a part of the previous figure showing cytoplasmic vacuolation of some mitral nerve cells (→) (H&E, Mic. Mag. 1000×).

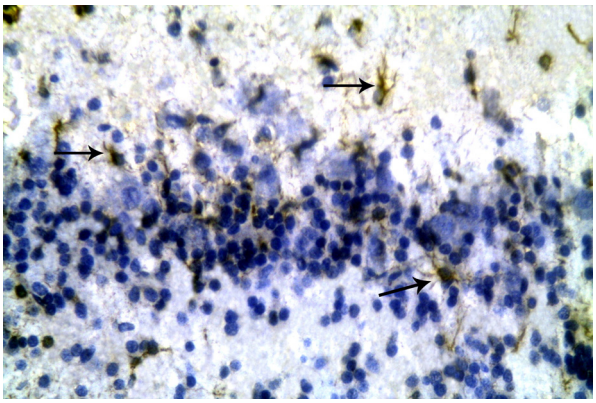

Fig. 11. A photomicrograph of a section in the olfactory bulb from group IV showing a few cells with positive immunoreaction in their processes in different layers (→) (immunostaining for GFAP, Mic. Mag. 400×).

stained cytoplasm and dark pyknotic peripheral nuclei (Figs. 6 and 7). Pericellular spaces were also observed around some mitral cells (Fig. 7). The granular cell layer appeared disorganized with loss of normal arrangement of the granule nerve cells (Fig. 6). The surrounding neuropil showed vacuolar spaces (Figs. 5–7).

GFAP-immunostained sections showed a strong extensive immunoreaction in the processes of astrocytes in different layers of the olfactory bulb (Fig. 8).

In animals treated with both meloxicam and $MnCl_2$ (group IV), mild structural changes were occasionally observed in some specimens such as cytoplasmic vacuolation of some mitral nerve cells (Figs. 9 and 10). In addition, few cells with positive GFAP immunoreactions in their cytoplasmic processes were observed in different layers (Fig. 11).

3.2. Electron microscopic results

Examination of ultrathin sections of the olfactory bulb from the control group showed normal mitral nerve cells with elongated perikaryon containing a central euchromatic nucleus and abundant cytoplasm containing RER, free ribosomes and mitochondria (Fig. 12). The granule nerve cells appeared smaller than mitral cells with scanty cytoplasm and heterochromatic nuclei (Fig. 13). The surrounding neuropil showed some unmyelinated nerve fibers and some myelinated axons with regular myelin sheaths (Figs. 12 and 13).

Meloxicam-treated group (group II) showed more or less the same ultrastructural appearance as the control group.

In $MnCl_2$-treated animals (group III), the mitral nerve cells showed prominent ultrastructural alterations such as cytoplasmic vacuolation (Figs. 14 and 15), accumulation of lysosomal dense bodies (Fig. 14), and swelling of mitochondria with disruption of the cristae (Fig. 16). In some specimens, blebbing of the nuclear envelope was also observed (Fig. 15). Some cells contained shrunken irregular nuclei with dilatation of perinuclear space (Fig. 16). However, the ultrastructural appearance of the granule nerve cells appeared more or less normal. Marked swelling and irregularity of some nerve fibers were also observed (Figs. 15–17). Some axons contained swollen mitochondria (Fig. 15) with splitting, corrugation and irregularity of the surrounding myelin sheaths (Figs. 15–17).

In contrast, these ultrastructural changes were much less pronounced in mitral nerve cells of group IV. The majority of mitral nerve cells appeared containing normal euchromatic nuclei, RER, free ribosomes and mitochondria. However, some axons showed mild splitting of the myelin sheath (Fig. 18).

Table 1
The mean values of area percentage of GFAP immunoreaction (mean ± SD) in different groups and their relations.

Groups	Area percentage of GFAP immunoreaction	*P*	Significance
Group I	1.32 ± 0.1		
Group II	1.37 ± 0.05	>0.05	Non-significant
Group III	3.62 ± 0.2	<0.001	Highly significant
Group IV	1.39 ± 0.01	>0.05	Non-significant

3.3. Morphometric analysis

Regarding GFAP immunoreaction, the mean value of area percentage of the positive reaction in group I (control group) was 1.32 ± 0.1 and that of group II was 1.37 ± 0.05 with a non-significant difference ($P > 0.05$) between them. The mean value of area percentage of the positive reaction in group III was 3.62 ± 0.2 recording a highly significant increase ($P < 0.001$) when compared with the control group, whereas that of group IV was 1.39 ± 0.01 recording a non-significant increase ($P > 0.05$) when compared with the control group (Table 1).

4. Discussion

The present work showed that administration of $MnCl_2$ induced structural changes in the olfactory bulb of adult albino rat in the form of loss of normal laminar organization, distortion of mitral and granule nerve cells, shrinkage of mitral cells with darkly stained cytoplasm and dark

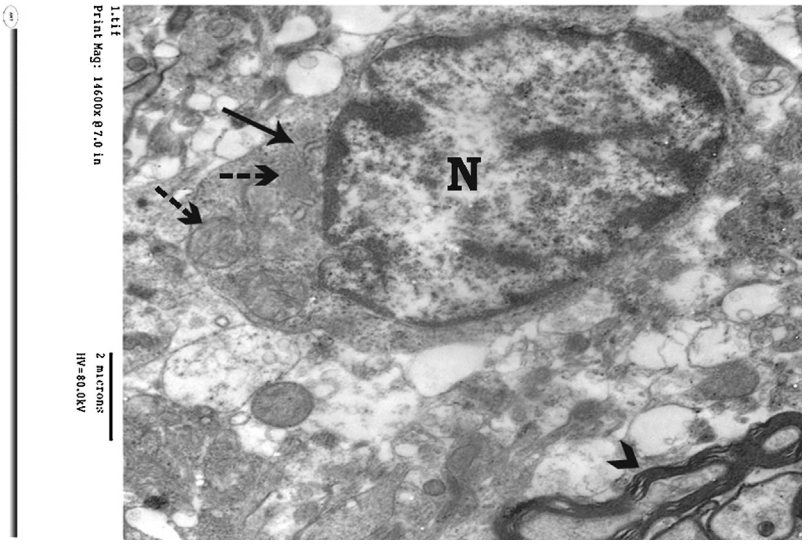

Fig. 12. An electron micrograph of the olfactory bulb from the control group showing a mitral nerve cell with an euchromatic nucleus (N) and abundant cytoplasm containing RER, free ribosomes (→) and mitochondria (—>). The surrounding neuropil contains some myelinated axons with regular myelin sheaths (>) (Mic. Mag. 14,600×).

pyknotic peripheral nuclei as well as pericellular spaces and vacuolar spaces in the surrounding neuropil.

Several studies have shown that the olfactory bulb is one of the brain regions with the highest Mn concentration [23,24]. It represents an important route for Mn transport, storage, and release in the brain, via a retrograde mechanism [25]. It has been shown that Mn may be taken by the olfactory neurons, released near their terminals, and is then transported to the olfactory cortex [26]. Another research has also demonstrated bilateral trans-synaptic Mn transport to other neurons of the olfactory system [27]. The connections of olfactory bulb with the brain limbic region suggested the possibility that in humans, the initial psychiatric symptoms of Mn poisoning may originate in the olfactory–limbic pathway [28,29].

It was reported that Mn exerts various effects at multiple sites within the central and peripheral nervous systems [30]. It disturbs the functions of basal ganglia as well as cortical brain regions, such as the hippocampus, frontal cortex and parietal cortex. Within the peripheral nervous system, Mn exerts its effect on motor nerves and neuromuscular junctions [3]. Mn was also shown to induce neuronal degeneration of caudate nucleus, putamen, globus pallidus, cerebellum and substantia nigra along with morphological alterations in the neurons from frontal cortex, hippocampus, midbrain and pons [31].

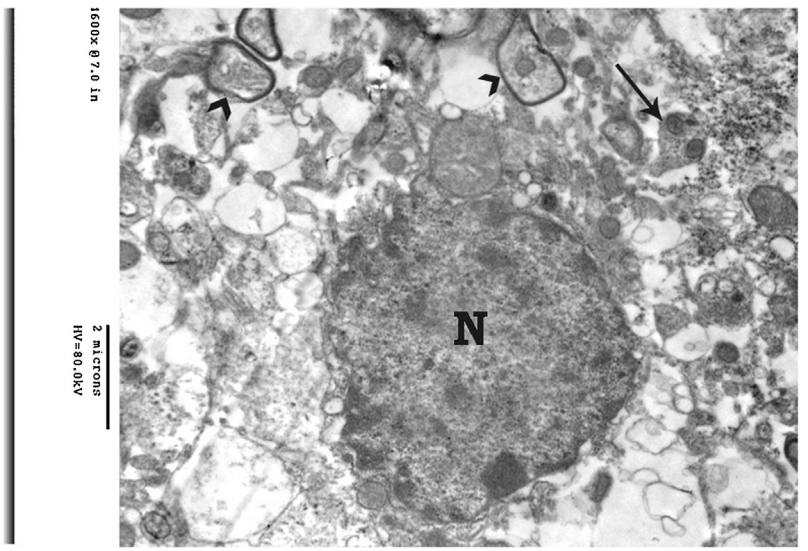

Fig. 13. An electron micrograph of the olfactory bulb from the control group showing a granule nerve cell with scanty cytoplasm and a heterochromatic nucleus (N). The surrounding neuropil contains some unmyelinated nerve fibers (→) and some myelinated axons with regular myelin sheaths (>) (Mic. Mag. 14,600×).

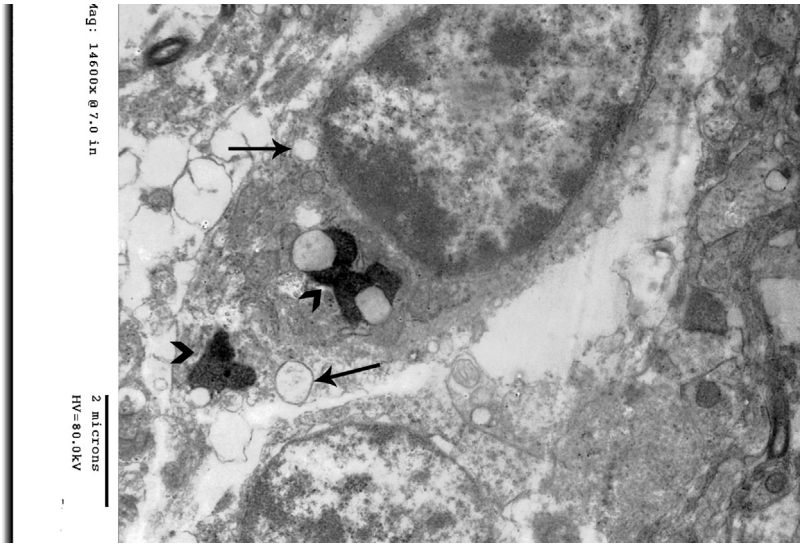

Fig. 14. An electron micrograph of the olfactory bulb from $MnCl_2$-treated group (group III) showing a mitral nerve cell with cytoplasmic vacuolation (→) and lysosomal dense bodies (>) (Mic. Mag. 14,600×).

Both in vivo and in vitro experiments suggested that oxidative stress and neuroinflammation are key mediators of Mn-induced neurodegeneration [32,33].

Regarding oxidative stress, it was found that the olfactory bulb is highly affected by chronic exposure to Mn as it is very sensitive to the oxidative stress induced by elevated concentrations of this metal [28,29]. Several studies indicated that oxidative stress, as an outcome of reactive oxygen species (ROS) accumulation, plays a major role in Mn-induced neurotoxicity. It was suggested that two possible mechanisms may lead to oxidative stress: interference with normal mitochondrial respiration and/or oxidation of dopamine and other catecholamines [32,34,35].

It is known that glutathione (GSH) is critical for protecting the cells from oxidative stress because it functions directly in reducing hydrogen peroxide and lipid peroxide levels [36]. Significant reduction in GSH levels has been observed in rat brain after exposure to Mn [17].

The other possible mechanism for Mn-induced neurodegeneration was neuroinflammation which was considered as a neurodegenerative disease characterized by increased prostaglandin (PGE2) levels [37]. In vitro studies have established the release of pro-inflammatory mediators in response to Mn [32]. Similarly, in mice exposed to Mn in vivo, levels of neuroinflammatory mediators and brain prostaglandins (PGEs) were increased [33].

Fig. 15. An electron micrograph of the olfactory bulb from group III showing a mitral nerve cell with cytoplasmic vacuolation (→) and blebbing of nuclear envelope (*). The surrounding neuropil contains swollen irregular axons that contain swollen mitochondria (—>) with corrugation of the myelin sheaths (>) (Mic. Mag. 17,500×).

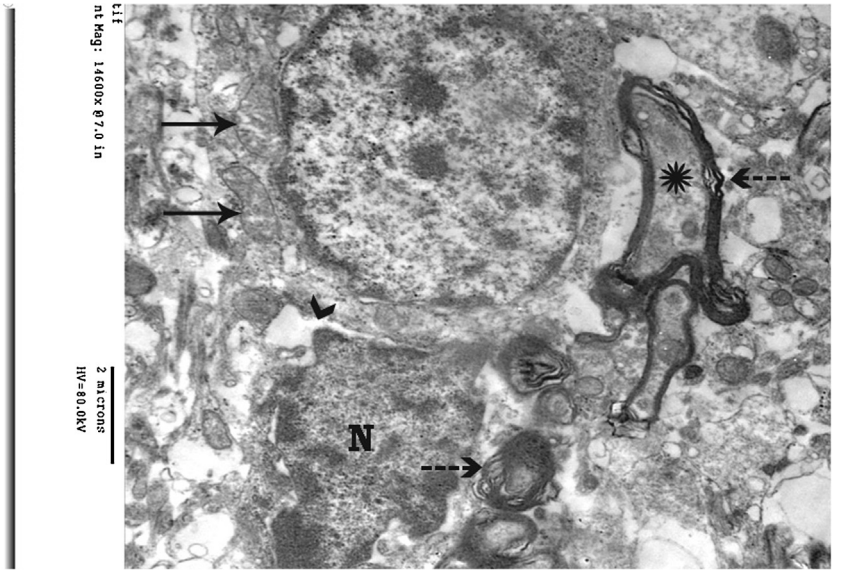

Fig. 16. An electron micrograph of the olfactory bulb from group III showing two mitral nerve cells: one contains swollen mitochondria with disrupted cristae (→) and the other shows a shrunken irregular nucleus (N) with dilatation of perinuclear space (>). The surrounding neuropil contains swollen irregular axons (*) with splitting and irregularity of the myelin sheaths (—>) (Mic. Mag. 14,600×).

In inflammatory conditions, the two enzymes that contribute to PGE2 production are cyclo-oxygenase-2 (COX-2) and microsomal PGE2 synthase-1 [37]. The involvement of these two enzymes in neurodegenerative diseases has been extensively demonstrated [38,39]. The cyclo-oxygenase-catalyzed reactions characteristic of inflammatory responses also produces ROS. Accordingly, a relationship exists between changes in biomarkers of oxidative damage and biomarkers of neuroinflammation [32].

The present work also showed ultrastructural alterations in the mitral nerve cells of $MnCl_2$-treated rats such as cytoplasmic vacuolation, lysosomal dense bodies, swelling of mitochondria with disruption of the cristae as well as nuclear changes such as shrinkage and irregularity of the nuclei with dilatation of perinuclear space and blebbing of the nuclear envelope. These observations come in agreement with the findings of previous studies that showed degenerated neurons with disorganization of cytoplasmic components and swelling of mitochondria in Mn-treated mice [6]. These findings were also similar to those observed by other investigators in the neurons of rat cerebral cortex after treatment with Mn, including cytoplasmic vacuolation, swollen mitochondria, dilated RER and Golgi apparatus as well as accumulated lysosomes [40].

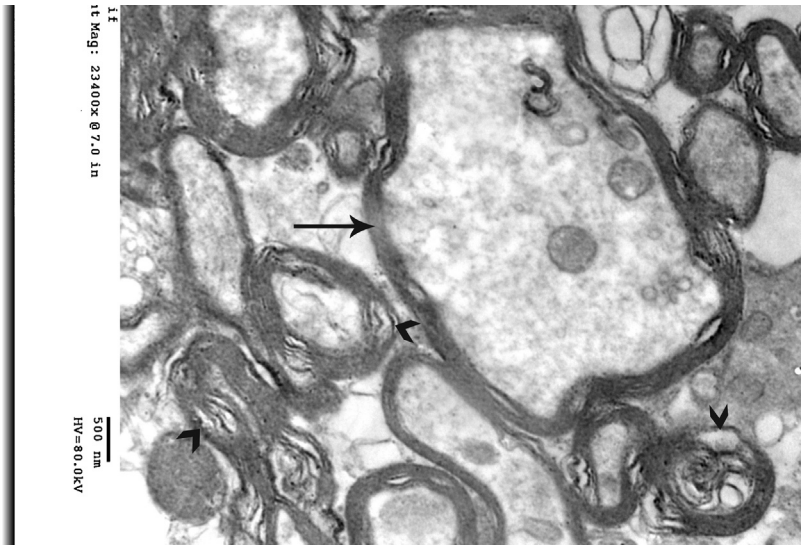

Fig. 17. An electron micrograph of the olfactory bulb from group III showing marked swelling and irregularity of some nerve axons (→) with splitting and irregularity of the surrounding myelin sheaths (>) (Mic. Mag. 23,400×).

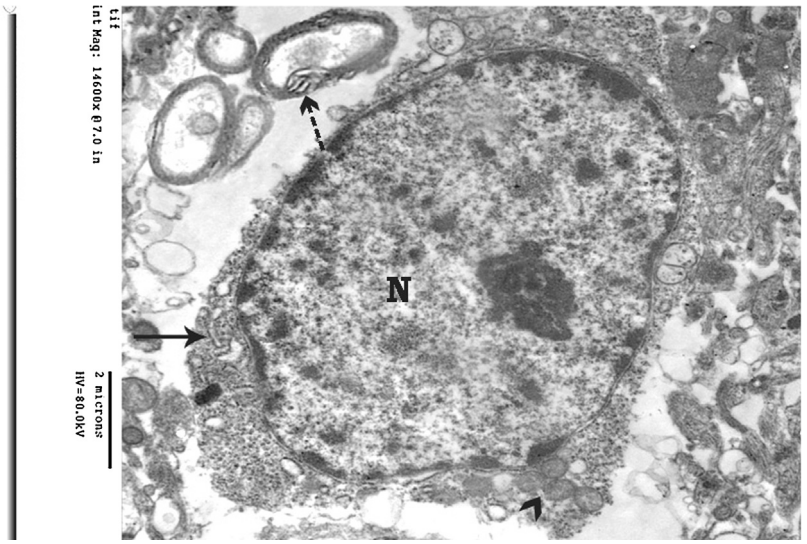

Fig. 18. An electron micrograph of the olfactory bulb from meloxicam and $MnCl_2$-treated group (group IV) showing a mitral nerve cell with an euchromatic nucleus (N), normal RER (→), free ribosomes and mitochondria (>). Some axons show mild splitting of the myelin sheath (—>) (Mic. Mag. 14,600×).

The cytoplasmic vacuoles observed in this study could be attributed to affection of the fluidity of the cell membrane by Mn [41]. In addition, the important role of Mn in the regulation of the interaction between intracellular membranes or vesicles and the cytoskeleton was suggested [42].

It was suggested that lysosomes could play an important role in Mn metabolism and the development of this metal toxicity [6]. It was also reported that Mn is accumulated in mitochondria and mitochondria-rich tissues in vivo. Therefore, this organelle could play an important role in the neurotoxicity of manganese [43]. Experimental evidence indicated that this metal caused neuronal degeneration secondary to an alteration of the oxidative energetic metabolism [6]. Changes in oxidative metabolism caused by Mn have been linked to cell apoptosis [44].

In this work, marked swelling and irregularity of nerve fibers were also observed in the olfactory bulb of $MnCl_2$-treated animals. Some axons contained swollen mitochondria with splitting, corrugation and irregularity of the surrounding myelin sheaths. These findings coincided with a previous study that showed alteration of the periodic pattern of myelin in Mn-treated mice [6]. Mitochondrial degeneration was also observed in the synapses of neurons in rat cerebral cortex after treatment with Mn [40].

As regards immunohistochemical results, the present work showed a highly significant increase in the area percentage of GFAP immunoreaction that was observed in the cytoplasmic processes of astrocytes in different layers of the olfactory bulb from $MnCl_2$-treated animals. In line with this finding, astrocytosis as well as ultrastructural changes in the astrocytes were previously observed in the olfactory bulb of Mn-treated mice [6]. In addition, an increased astrocyte phagocytic activity associated with ultrastructural changes in the astrocytes, oligodendrocytes and microglia were previously reported in the caudate nucleus, substantia nigra and cerebral cortex of Mn-treated rats [45].

It was reported that GFAP is an intermediate filament protein found in the cytoskeleton of astroglia. It may serve as a serum marker that is released after central nervous system cell damage subsequent to astrogliosis [16].

It was found that astrocytes respond to all forms of neurodegenerative diseases by a process commonly referred to as reactive astrogliosis, which involves changes in their molecular expression, upregulation of GFAP, cellular hypertrophy, proliferation and scar formation. Molecular mediators of reactive astrogliosis can be released by different cell types in CNS tissue including neurons, microglia, oligodendrocytes, endothelial cells, leukocytes and other astrocytes, in response to CNS insults [46].

Several studies indicated that reactive astrocytes can protect neuronal cells and tissue from oxidative stress via glutathione production and by restricting the spread of inflammation as well as stabilizing extracellular fluid and ion balance. These findings indicate that reactive astrocytes can exert a range of essential neuroprotective and repair-related functions in response to CNS insults of various kinds. However, under certain circumstances, astrogliosis can also lead to harmful effects through scar formation and loss of normal functions [47,48].

In animals concomitantly treated with both meloxicam and $MnCl_2$, mild structural changes were occasionally observed in some specimens, such as cytoplasmic vacuolation of some mitral nerve cells and mild splitting of the myelin sheaths in some axons, indicating that meloxicam could ameliorate the structural changes induced by $MnCl_2$.

Several anti-inflammatory agents have been found to reduce Mn neurotoxicity [3]. This could be related to the report that the inflammatory processes play a role in the pathogenesis of Mn-induced toxicity [32,33].

It was also shown that meloxicam has antioxidant like properties as it reduced free oxygen radicals and lipid peroxidation in the brain of aluminum-treated rats [14].

It was also found to reduce oxygen radical generation in rat gastric mucosa [49]. Although the exact mechanism of action is unknown, many investigators have shown that the NSAIDs could eliminate the active oxygen species particularly superoxide anion [12]. Moreover, the circulating superoxide dismutase levels were improved with NSAID treatment in rheumatoid arthritis [13].

Meloxicam has been reported to cross the blood brain barrier [50]. Subsequently, it may gain access to brain parenchymal Mn ions and directly decrease the bioavailability of brain Mn and its targeting sensitive sites [51].

In conclusion, $MnCl_2$ could induce structural changes in the olfactory bulb of adult albino rat. These changes could be partially minimized by concomitant administration of meloxicam.

Conflict of interest

None declared.

References

[1] Lucchini RG, Martin CJ, Doney BC. From manganism to manganese-induced parkinsonism: conceptual model based on the evolution of exposure. Neuromol Med 2009;11:311–21.

[2] Aschner M, Lukey B, Tremblay A. The Manganese Health Research Program (MHRP): status report and future research needs and directions. Neurotoxicology 2006;27:733–6.

[3] Marreilha dos Santos AP, Lucas RL, Andrade V, Mateus ML, Milatovic D, Aschner M, et al. Protective effects of ebselen (Ebs) and para-aminosalicylic acid (PAS) against manganese (Mn)-induced neurotoxicity. Toxicol Appl Pharmacol 2012;258:394–402.

[4] Santamaria AB. Manganese exposure, essentiality and toxicity. Indian J Med Res 2008;128:484–500.

[5] Bowler RM, Nakagawa S, Drezgic M, Roels HA, Park RM, Diamond E, et al. Sequelae of fume exposure in confined space welding: a neurological and neuropsychological case series. Neurotoxicology 2007;28:298–311.

[6] Villalobos V, Bonilla E, Castellano A, Novo E, Caspersen R, Giraldoth D, et al. Ultrastructural changes of the olfactory bulb in manganese treated mice. Biocell 2009;33(3):187–97.

[7] Dobson AW, Erikson KM, Aschner M. Manganese neurotoxicity. Ann N Y Acad Sci 2004;1012:115–28.

[8] Erikson KM, Dorman DC, Lash LH, Aschner M. Manganese inhalation by rhesus monkeys is associated with brain regional changes in biomarkers of neurotoxicity. Toxicol Sci 2007;97:459–66.

[9] Huang C, Chu N, Lu C, Chen R, Calne D. Long-term progression in chronic manganism. Neurology 1998;50:698–700.

[10] Kim EA, Cheong HK, Choi DS, Sakong J, Ryoo JW, Park I, et al. Effect of occupational manganese exposure on the central nervous system of welders: ^{1}H magnetic resonance spectroscopy and MRI findings. Neurotoxicology 2007;28(2):276–83.

[11] Del Tacca M, Colucci R, Fornai M, Blandizzi C. Efficacy and tolerability of meloxicam, a COX-2 preferential nonsteroidal anti-inflammatory drug: a review. Clin Drug Invest 2002;22:799–818.

[12] Kimura K. Mechanism of active oxygen species reduction by non-steroidal anti-inflammatory drugs. Int J Biochem Cell Biol 1997;29(3):437–46.

[13] Nivsarkar M. Improvement in circulating superoxide dismutase levels: role of nonsteroidal anti-inflammatory drugs in rheumatoid arthritis. Biochem Biophys Res Commun 2000;270(3):714–6.

[14] Nivsarkar M, Banerjee A, Shah D, Trivedi J, Patel M, Cherian B, et al. Reduction in aluminum induced oxidative stress by meloxicam in rat brain. Iran Biomed J 2006;10(3):151–5.

[15] Standring S, Ellis H, Healy JC, Johnson D, Williams A, Collins P, et al. Gray's anatomy: the anatomical basis of clinical practice. 40th ed. London: Churchill Livingstone, Elsevier; 2008. p. 1030.

[16] Lumpkins KM, Bochicchio GV, Keledjian K, Simard JM, McCunn M, Scalea T. Glial fibrillary acidic protein is highly correlated with brain injury. J Trauma 2008;65(4):778–82.

[17] Marreilha dos Santos AP, Lopes Santos M, Batoreu MC, Aschner M. Prolactin is a peripheral marker of manganese neurotoxicity. Brain Res 2011;1382:282–90.

[18] Wakuta M, Morishige N, Chikama T, Seki K, Nagano T, Nishida T. Delayed wound closure and phenotypic changes in corneal epithelium of the spontaneously diabetic Goto-Kakizaki rat. Investig Ophthalmol Vis Sci 2007;48:590–6.

[19] Bancroft JD, Gamble M. Theory and practice of histological techniques. 6th ed. China: Churchill Livingstone, Elsevier; 2008. p. 83.

[20] Machado GF, Alessi AC. Glial fibrillary acidic protein (GFAP) immunoreactive astrocytes in the CNS of normal and rabies-infected adult cattle. I. Hippocampus and dentate gyrus. Braz J Vet Res Anim 1997;34(6):345–8.

[21] Ramos-Vara JA, Kiupel M, Baszler T, Bliven L, Brodersen B, Chelack B, et al. Suggested guidelines for immunohistochemical techniques in veterinary diagnostic laboratories. J Vet Diagn Invest 2008;20:393–413.

[22] Bozzola JJ, Russell LD. Electron microscopy: principles and techniques for biologists. 2nd ed. London: Jones and Bartlett Publishers; 1999. p. 16.

[23] Normandin L, Carrier G, Gardiner P, Kennedy G, Hazell A, Mergler D, et al. Assessment of bioaccumulation, neuropathology, and neurobehavior following subchronic (90 days) inhalation in Sprague-Dawley rats exposed to manganese phosphate. Toxicol Appl Pharmacol 2002;183:135–45.

[24] Normandin L, Hazell A. Manganese neurotoxicity: an update of pathophysiologic mechanisms. Metab Brain Dis 2002;17:375–87.

[25] Dorman D, Brenneman K, Mcelveen A, Lynch S, Wong B. Olfactory transport: a direct route of delivery of inhaled manganese phosphate to the rat brain. J Toxicol Environ Health 2002;65:1493–511.

[26] Henriksson J, Tallkvist J, Tjalve H. Transport of manganese via the olfactory pathway in rats: dosage dependency of the uptake and subcellular distribution of the metal in the olfactory epithelium and the brain. Toxicol Appl Pharmacol 1999;156:119–28.

[27] Cross D, Minoshima S, Anzai Y, Flexman J, Keogh B, Kim Y, et al. Statistical mapping of functional olfactory connections of the rat brain in vivo. NeuroImage 2004;23:1326–35.

[28] Dobson A, Weber S, Dorman D, Lash L, Erikson K, Aschner M. Oxidative stress is induced in the rat brain following repeated inhalation exposure to manganese sulfate. Biol Trace Elem Res 2003;93:113–26.

[29] Erikson K, Dorman D, Lash L, Aschner M. Persistent alterations in biomarkers of oxidative stress resulting from combined in utero and neonatal manganese inhalation. Biol Trace Elem Res 2005;104:151–64.

[30] Finkelstein Y, Milatovic D, Aschner M. Modulation of cholinergic systems by manganese. Neurotoxicology 2007;28:1003–14.

[31] Yamada M, Ohno S, Okayasu Y, Okeda R, Hatakeyama S, Watanabe H, et al. Chronic manganese poisoning: a neuropathological study with determination of manganese distribution in the brain. Acta Neuropathol 1986;70:273–8.

[32] Milatovic D, Milatovic SZ, Gupta RC, Yu Y, Aschner M. Oxidative damage and neurodegeneration in manganese-induced neurotoxicity. Toxicol Appl Pharmacol 2009;240:219–25.

[33] Sriram K, Lin GX, Jefferson AM, Roberts JR, Chapman RS, Chen BT, et al. Dopaminergic neurotoxicity following pulmonary exposure to manganese-containing welding fumes. Arch Toxicol 2010;84(7):521–40.

[34] Zhang S, Fu J, Zhou Z. In vitro effect of manganese chloride exposure on reactive oxygen species generation and respiratory chain complexes activities of mitochondria isolated from rat brain. Toxicol In Vitro 2004;18:71–7.

[35] Yin Z, Aschner JL, dos Santos AP, Aschner M. Mitochondrial-dependent manganese neurotoxicity in rat primary astrocyte cultures. Brain Res 2008;8(1203):1–11.

[36] Erikson KM, Dorman DC, Lash LH, Dobson AW, Aschner M. Airborne manganese exposure differentially affects end points of oxidative stress in an age and sex-dependent manner. Biol Trace Elem Res 2004;100(1):49–62.

[37] Matsumura K, Kobayashi S. Signaling the brain in inflammation: the role of endothelial cells. Front Biosci 2004;9:2819–26.

[38] Chaudhry UA, Zhuang H, Crain BJ, Doré S. Elevated microsomal prostaglandin-E synthase-1 in Alzheimer's disease. Alzheimers Dement 2008;4(1):6–13.

[39] Wendeburg L, Pinheiro de Oliveira AC, Bhatia HS, Candelario-Jalil E, Fiebich BL. Resveratrol inhibits prostaglandin formation in IL-1β-stimulated SK-N-SH neuronal cells. J Neuroinflamm 2009;14:6–26.

[40] Bikashvili T, Shukakidze A, Kikniadze G. Change in the ultrastructure of the rat cerebral cortex after oral doses of manganese chloride. Neurosci Behav Physiol 2001;31:385–9.

[41] Kumar R, Srivastava S, Ashok K, Seth P. Alteration in some membranes in rat brain following exposure to manganese. Pharmacol Toxicol 1996;79:47–8.

[42] Towler M, Prescott A, James J, Lucocq J, Ponnambala M. The manganese cation disrupts membrane dynamics along the secretory pathway. Exp Cell Res 2000;259:167–79.
[43] Gavin C, Gunter K, Gunter T. Mn^{2+} sequestration by mitochondria and inhibition of oxidative phosphorylation. Toxicol Appl Pharmacol 1992;115:1–5.
[44] Hirata Y, Kayo A, Kazutoshi K. Activation of JNK pathway and induction of apoptosis by manganese in PC12 cells. J Neurochem 1998;71:1607–15.
[45] Shukakidze A, Lazriev I, Khetsuriani R, Bikashvili T. Changes in the ultrastructure of neuroglia in some regions of the rat brain in manganese chloride poisoning. Morfologiia 2001;120:35–41 [abstract].
[46] Sofroniew MV. Molecular dissection of reactive astrogliosis and glial scar formation. Trends Neurosci 2009;32(12):638–47.
[47] Vargas MR, Johnson DA, Sirkis DW, Messing A, Johnson JA. Nrf2 activation in astrocytes protects against neurodegeneration in mouse models of familial amyotrophic lateral sclerosis. J Neurosci 2008;28:13574–81.
[48] Sofroniew MV, Vinters HV. Astrocytes: biology and pathology. Acta Neuropathol 2010;119:7–35.
[49] Villegas I, Martin MJ, La Casa C, Motilva V, Alarcon de la Lastra C. Effects of meloxicam on oxygen radical generation in rat gastric mucosa. Inflamm Res 2000;49(7):361–6.
[50] Jollict P, Simon N, Brce F, Urien S, Pagliara A, Carrupt PA, et al. Blood-to-brain transfer of various oxicams: effect of plasma binding on their brain delivery. Pharm Res 1997;14(5):650–6.
[51] Zheng W, Jiang YM, Zhang Y, Jiang W, Wang X, Cowan DM. Chelation therapy of manganese intoxication with para-aminosalicylic acid (PAS) in Sprague-Dawley rats. Neurotoxicology 2009;30:240–8.